

# Introduction

This chapter starts with a brief historical overview of the neutrinos in Section 1.1, which is the system under consideration in this thesis. In Section 1.2, a succinct description of the Standard Model (SM) is provided along with its fundamental gauge group and particle spectrum. The concept of particle mixing in the SM framework is also described. Next, in the Subsection 1.2.1 several drawbacks of SM are discussed. In Subsection 1.2.2 the properties of neutrino in SM is elucidated along with its importance as a probe to explore physics beyond SM (BSM). The concept of particle mixing in the neutrino sector is introduced in Section 1.3 with a detailed discussion of neutrino oscillation. In Subsection 1.3.1 the history of the neutrino oscillation is briefly depicted, followed by the description of oscillation phenomenon in the vacuum and SM matter effect in the Subsections 1.3.2 and 1.3.3 respectively. Some information of the current neutrino oscillation experiments is also comprehended in Subsection 1.3.4. Further, the brief outline of the thesis is mentioned in Section 1.4.

## 1.1 Historical background

The origin of neutrino physics dates back to the discovery of radioactivity by Henry Becquerel in 1896 during the study of the X-rays. Later Rutherford discovered two different kinds of particles namely,  $\alpha$  and  $\beta$  produced as the byproducts of the radioactive elements. The  $\gamma$ -ray was discovered later in 1900. In 1914, it was pointed out by James Chadwick that the nature of the  $\beta$ -spectra, which was then assumed to be a two-body decay process, was continuous unlike the discrete spectra observed for  $\alpha$  and  $\gamma$ -decay. The observation of the continuous  $\beta$ -spectra was contradictory with the law of energy conservation apparently. In addition, the angular momentum was also not conserved in the interaction. At this point, it was suggested by Niels Bohr that the conservation of energy might be only possible in the statistical description *i.e.* energy might not be conserved in each individual decay process. In order to explain the missing energy in  $\beta$ -decay, in 1930 Wolfgang Pauli came up with the *Neutrino hypothesis* in which he mentioned the emission of an additional electrically neutral particle in the  $\beta$ -decay. At that time this particle was named *neutron* having a mass of the order of an electron mass. However, after the discovery of the neutron in 1932, this particle was renamed as *neutrino* by Enrico Fermi. The apparent absurdity in the continuous  $\beta$ -spectrum is now resolved as the energy difference between the initial and final nuclei is shared between the  $\beta$ -particle and neutrino. Also, for the requirement of the conservation of spin angular momentum, the neutrino had to be a spin-1/2 particle. In 1933 Fermi concluded that the neutrino is massless and in 1934 he established the theory of  $\beta$ -decay [1] which was then realized as a point interaction.

Fermi's theory was the first breakthrough in the theory of weak interaction in which the nuclear spin remained unchanged. However, in some of the  $\beta$ -decay processes the nuclear spins of the initial and final nuclei was found to be differed by one unit. In order to explain this, Fermi's theory of  $\beta$ -decay was further extended by George Gamow and Edward Teller, who incorporated the axial vector currents by maintaining the parity conservation [2], since at that time the parity

symmetry was considered to be universal. In 1934 Hans Bethe and Rudolf Peierls gave an estimation of the strength of the weak interaction [3] which was extremely small. This made the physicists to believe that it might not be possible to observe the neutrino in experiment. However, in 1956 Reines and Cowan discovered the neutrino in a reactor experiment using a large flux of anti-neutrino [4,5].

Different properties of the neutrino were further discovered in the following years. As mentioned previously, it was assumed earlier that parity was conserved in all processes including the weak interaction. However, after the discovery of the violation of parity symmetry in the weak decay of  $K$ -meson, known as the  $\tau - \theta$  puzzle, the parity violation was also tested in other weak processes. In 1956 the parity violation was confirmed in the  $\beta$ -decay of polarized  $^{60}\text{Co}$  [6]. Later, in 1958 the constant helicity of the neutrino was measured in the famous Goldhaber-experiment [7].

In the meantime, the muons ( $\mu$ ) were discovered in 1937 by J. Street and E. Stevenson [8,9]. Decay of  $\mu$  was discovered in 1941 into electron and the energy spectrum was found to be continuous. This resulted in the conclusion in 1948 that  $\mu$  decay is also a three-body process similar to the  $\beta$ -decay. This led to the prediction of a second kind of neutrino  $\nu_\mu$ . After this the universality of the Fermi interaction of the electrons and muon was established by Pontecorvo [10]. This raised the concept of different lepton generations and their corresponding lepton numbers ( $L_e$  and  $L_\mu$ ). In 1962 the existence of  $\nu_\mu$  was confirmed at Brookhaven National Laboratory (BNL) [11]. Meanwhile, in 1957 the current  $V - A$  theory of the weak interaction was established by Gell-Mann and Feynman by using the two-component formalism of the massless neutrino [12]. In this theory the neutrino and anti-neutrino have left and right handed helicity respectively which automatically results in  $V - A$  coupling. Finally, the prediction of the third kind of neutrino  $\nu_\tau$  was realized just after the discovery of the  $\tau$ -lepton in 1970 at SLAC. The tau neutrino  $\nu_\tau$  was observed in DONUT collaboration in 2000 at Fermilab [13].

## 1.2 Standard Model

The three fundamental forces of the Universe, namely strong, electromagnetic (EM) and weak interactions are described by the Standard Model of particle physics. Developed in the later part of the 20th century the SM is the most successful theory of nature at present. With the discovery of non-Abelian gauge theory by Yang Chen-Ning and Robert Mills in 1954 [14] and the non-conservation of the parity symmetry in weak interaction in 1957 [6], the development of the unification of the electromagnetic and weak force by Sheldon Glashow in 1961 [15] and the incorporation of Higgs mechanism [16–21] developed in 1964 into the electroweak unification formalism in the year of 1967, by Steven Weinberg [22] and Abdus Salam [23], the modern theory of SM was finally established.

Further, after the discovery of the weak neutral current at CERN in 1973 [24,25], the theory of electroweak unification was widely accepted for which Glashow, Weinberg and Salam received Nobel Prize in 1979. The theory of strong interaction was developed in 1974 with the establishment of the theory of asymptotic freedom. At last, with the discovery of the Higgs boson in 2012 at CERN [26,27] the complete picture of the SM describing the three fundamental interactions of nature was finally confirmed.

The fundamental building blocks of matter are the fermions, namely quarks and leptons in the SM. There are six quarks, up ( $u$ ), down ( $d$ ), charm ( $c$ ), strange ( $s$ ), top ( $t$ ), bottom ( $b$ ). The three of the leptons are electrically charged which are electron ( $e$ ), muon ( $\mu$ ) and tau ( $\tau$ ), while the three neutrinos ( $\nu_e$ ,  $\nu_\mu$ ,  $\nu_\tau$ ) are electrically neutral. Each fermion has its corresponding anti-fermion. The quarks can contribute to all three fundamental interactions. The charged leptons ( $e$ ,  $\mu$ ,  $\tau$ ) take part in EM and weak interactions and the neutrinos are only involved in the weak

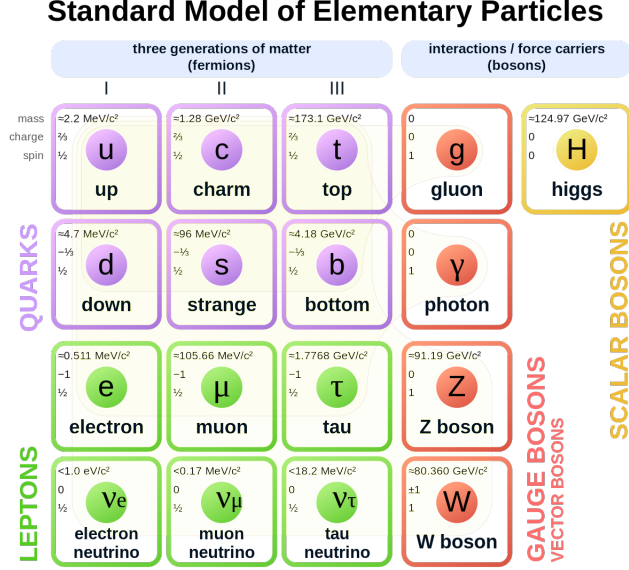


Figure 1.1: Particle content of the SM

processes. In SM the fermions appear in three generations, which is illustrated in Fig. 1.1.

Mathematically the SM is a renormalizable non-Abelian quantized Yang-Mills theory [28, 29], invariant under the symmetry group  $SU(3)_C \otimes SU(2)_L \otimes U(1)_Y$ . The  $SU(3)_C$  gauge group corresponds to eight massless gluons ( $g$ ) which carry the colour charge ( $C$ ) in the strong interaction. The electroweak (EW) group  $SU(2)_L \otimes U(1)_Y$  has four mediators: the massive vector bosons  $W^\pm$ ,  $Z^0$  which mediate the weak interaction and the massless photon ( $\gamma$ ) which is the mediator of the EM interaction. The local symmetry group  $SU(2)_L$  corresponds to weak isospin quantum number ( $I$ ) and it is a non-Abelian Lie group with three generators  $I_i (= \tau_i/2)$ , given by

$$\left[ \frac{\tau_a}{2}, \frac{\tau_b}{2} \right] = i\epsilon_{abc} \frac{\tau_c}{2}, \quad (1.1)$$

where  $\tau_i$  ( $i = 1, 2, 3$ ) are the Pauli matrices. The third component of weak isospin ( $I_3$ ) and the weak hypercharge ( $Y$ ), which is the generator of the  $U(1)_Y$  Abelian group, are connected by the following expression

$$Q = I_3 + \frac{Y}{2}.$$

Here  $Q$  is the electric charge. The  $SU(2)_L$  group allows weak interaction only among the left handed fermions. This is possible because of the  $V - A$  structure of weak interaction. The fermions with the left handed (LH) chirality are represented as weak isospin doublets

$$q_L = \begin{pmatrix} u \\ d \end{pmatrix}_L, \begin{pmatrix} c \\ s \end{pmatrix}_L, \begin{pmatrix} t \\ b \end{pmatrix}_L \quad (1.2)$$

$$l_L = \begin{pmatrix} e \\ \nu_e \end{pmatrix}_L, \begin{pmatrix} \mu \\ \nu_\mu \end{pmatrix}_L, \begin{pmatrix} \tau \\ \nu_\tau \end{pmatrix}_L. \quad (1.3)$$

The members of the doublets have different values of the third component of the isospin ( $I_3$ ). The right handed (RH) chiral fermions ( $q_R, l_R$ ) do not possess weak isospin charge, hence they are

Fermions	$SU_C(3) \otimes SU_L(2) \otimes U_Y(1)$ representation
Up type LH quark ( $u_L, c_L, t_L$ )	(3, 2, 1/3)
Down type LH quark ( $d_L, s_L, b_L$ )	(3, 2, 1/3)
Up type RH quark ( $u_R, c_R, t_R$ )	(3, 1, 4/3)
Down type RH quark ( $d_R, s_R, b_R$ )	(3, 1, -2/3)
LH charged lepton ( $e_L, \mu_L, \tau_L$ )	(1, 2, -1)
LH neutrino ( $\nu_{eL}, \nu_{\mu L}, \nu_{\tau L}$ )	(1, 2, -1)
RH charged lepton ( $e_R, \mu_R, \tau_R$ )	(1, 1, -2)

**Table 1.1:** SM gauge group representations of the quarks and leptons

singlets under  $SU(2)_L$ . The representation of the fermions under  $SU(3)_C \otimes SU(2)_L \otimes U(1)_Y$  group is illustrated in Table 1.1. The group of the colour charge  $SU(3)_C$  is an exact symmetry which makes the gluons massless. The  $SU(3)_C$  symmetry is unbroken and there is no mixing between the group of the colour charge with electroweak sector  $SU(2)_L \otimes U(1)_Y$ , hence  $SU(3)_C$  group can be studied independently.

The three generators of  $SU(2)_L$  are associated with three gauge bosons  $W_\mu^1, W_\mu^2$  and  $W_\mu^3$ , while the mediator field of  $U(1)_Y$  is denoted by  $B_\mu$ . The physical fields giving rise to the weak and EM interactions are generated from these four gauge fields through the process of *spontaneous symmetry breaking*, in which the EW symmetry  $SU(2)_L \times U(1)_Y$  is broken spontaneously to produce the EM symmetry  $U(1)_Q$  which is an unbroken symmetry. The charged gauge mediators of the weak interaction can be constructed from the linear combination  $W_\mu^\pm = (W_\mu^1 \mp iW_\mu^2)/\sqrt{2}$ . On the other hand, the weak neutral boson  $Z^0$  and the photon field  $A_\mu$  are obtained by performing a rotation in  $(W_\mu^3, B_\mu)$  plane, given by

$$\begin{aligned}
Z_\mu &= \cos\theta_w W_\mu^3 - \sin\theta_w B_\mu, \\
A_\mu &= \sin\theta_w W_\mu^3 + \cos\theta_w B_\mu.
\end{aligned}
\tag{1.4}$$

Here  $\theta_w$  is the weak mixing angle, known as the Weinberg angle.

In the SM the particles gain mass via Higgs mechanism after the spontaneous symmetry breaking. The three gauge bosons  $W^\pm$  and  $Z^0$  acquire mass but the photon remains massless. To implement this, a complex scalar weak doublet is introduced as,  $\Phi = (\phi^+, \phi^0)^T = (\phi_1 + i\phi_2, \phi_3 + i\phi_4)^T$ . Here  $\phi_1, \phi_2, \phi_3$  and  $\phi_4$  are the real fields. There are infinite degenerate solutions of  $\Phi^\dagger \Phi$ . If one specific solution is selected among them, the EW symmetry is spontaneously broken  $SU(2)_L \otimes U(1)_Y \rightarrow U(1)_Q$ . As the process of spontaneous symmetry breaking takes place, three real components of the Higgs doublet  $\Phi$  become massless Goldstone bosons which are absorbed in the physical fields  $W^\pm$  and  $Z^0$ . The fourth field associated with the  $U(1)_Q$  symmetry remains massless and is identified as the photon field. Due to the invariance of the vacuum under  $U(1)_Q$  transformation, the  $U(1)_Q$  group remains unbroken which implies that the  $U(1)_Q$  is a good symmetry of the vacuum. The fermions acquire mass by Yukawa interaction with the Higgs field.

Further, the concept of particle mixing was introduced in the quark sector by Nicola Cabibbo in 1963 [30] to restore the concept of lepton flavour universality in SM. He proposed that the quarks that contribute to the weak interactions are rotated by the Cabibbo angle. In the decay processes involving the transformation of  $d$  and  $s$  quarks into  $u$  quarks, the actual states coupling to the  $u$

quark are represented as

$$\begin{pmatrix} d' \\ s' \end{pmatrix} = \begin{pmatrix} \cos\theta_c & \sin\theta_c \\ -\sin\theta_c & \cos\theta_c \end{pmatrix} \begin{pmatrix} d \\ s \end{pmatrix}, \quad (1.5)$$

where  $\theta_c$  is the mixing angle. Thus, the actual form of the isospin doublet involved in the weak interaction is  $(u, d') = (u, d\cos\theta_c + s\sin\theta_c)^T$ . The state  $d'$  and  $d$  are understood as the weak and mass eigenstates. However, Cabibbo's theory was not sufficient to explain the very small branching ratio of the strangeness changing neutral current decay mode of the neutral kaon  $K_L \rightarrow \mu^+ + \mu^-$ . This problem was resolved by the incorporation of the additional charm quark ( $c$ ), which was not observed experimentally at that time. The  $c$  quark formed another weak isospin doublet  $(c, s')^T$ , so that the unitary mixing matrix, given by Eqn. (1.5) can be written as

$$\begin{pmatrix} \cos\theta_c & \sin\theta_c \\ -\sin\theta_c & \cos\theta_c \end{pmatrix} = \begin{pmatrix} V_{ud} & V_{us} \\ V_{cd} & V_{cs} \end{pmatrix}, \quad (1.6)$$

where the matrix element  $V_{ij}$  represents the coupling between the  $i$ -th and  $j$ -th quark. The inclusion of both of the weak doublets in the theory was able to generate the small branching ratio observed in the decay process which led to the conclusion that the strangeness changing weak decays are highly suppressed at the tree level in SM. This is known as the GIM mechanism, named after S. Glashow, J. Iliopoulos and L. Maiani [31].

The concept of mixing was further extended in the three generations of quarks by Kobayashi and Maskawa in 1973 [32], after the discovery of CP violation in 1964 in the neutral kaon decay by James Cronin and Val Filch. Since in the previous four quark model CP violation could not be explained, the mixing among three generations of quarks were considered in which the CP violation originates in terms of the complex phase in the mixing matrix. The  $3 \times 3$  unitary quark mixing matrix is given by

$$\begin{pmatrix} d' \\ s' \\ b' \end{pmatrix} = \begin{pmatrix} V_{ud} & V_{us} & V_{ub} \\ V_{cd} & V_{cs} & V_{cb} \\ V_{td} & V_{ts} & V_{tb} \end{pmatrix} \begin{pmatrix} d \\ s \\ b \end{pmatrix}. \quad (1.7)$$

Most of the elements of the CKM matrix are precisely measured. The value of  $|V_{ud}|$  is  $0.97420 \pm 0.00021$ , determined from the consideration of superallowed nuclear beta decays ( $0^+ \rightarrow 0^+$ ) [33]. The parameter  $|V_{us}|$  is extracted from the semi-leptonic kaon decay  $K \rightarrow \pi e \nu$ . Taking the average over five such decay modes considering the form factor at the zero momentum transfer,  $|V_{us}| = 0.2231 \pm 0.0008$ . The semi-leptonic decay of  $D$ -meson via  $D \rightarrow \pi l \nu$  constrains  $|V_{cd}| (= 0.2140 \pm 0.0029 \pm 0.0093)$  and  $|V_{cs}| (= 0.997 \pm 0.017)$  [34]. The elements  $|V_{ub}|$  and  $V_{cb}$  are estimated from the semi-leptonic  $B$ -meson decays.

The standard parametrization of the CKM mixing matrix contains three mixing angles and one phase corresponding to CP violation. The CP phase in the quark sector is the only source of CP violation in the SM. In case of  $n$  number of quark generations, the  $n \times n$  unitary mixing matrix is characterized by  $n^2 - (2n - 1) = (n - 1)^2$  number of parameters, out of which the number of angles is  $[n(n - 1)/2$  and  $(n - 1)^2 - n(n - 1)/2]$  represents the number of phases [35]. Therefore, for three generations of quarks, there are three angles and one phase which leads to the CP violation in the quark sector of the SM, as given by Eqn. (1.7). The CP violation among the leptons is not established yet. In the beyond SM scenario, there is mixing among the neutrino flavours which is understood in terms of a unitary transformation analogous to the CKM matrix. The parameter counting of the CKM parametrization is also applicable in the case of neutrino mixing.

### 1.2.1 Beyond Standard Model

Despite its astounding success over the decades in explicating several physical phenomena, the theory of SM is not the complete theory of nature. From a theoretical point of view, the SM

can be considered to be the lower energy manifestation of a full theory existing at some higher energy scale. Also, the necessity of new physics (NP) beyond the SM can be stipulated from several experimental evidences. There are several discrepancies incomprehensible within the SM framework which are discussed below.

- *Exclusion of gravity:* The SM is unable to incorporate gravity with the three other fundamental interactions. In the general theory of relativity, which is the most successful theory of gravity till date, gravity is described as the consequence of the curvature of space time, unlike the scenario of the SM in which a fundamental interaction is mediated by a gauge boson. Although, gravity is absurdly weak at the EW scale ( $\mathcal{O}(100)$  GeV) its strength is assumed to be equal with the other fundamental interactions at Planck scale ( $10^{19}$  GeV). In several BSM models the concept of extra dimensions is incorporated, in which the fundamental Planck scale can be brought down to the testable limits of the current experimental facilities. This is discussed in details in Chapter 2.
- *Dark matter and dark energy:* There is strong evidence from several astrophysical and cosmological backgrounds supporting the existence of the dark matter [36, 37] which contributes nearly 26.8% of the total matter content of the Universe. Dark energy is an unknown form of energy that covers about 68.3% of the total energy density of the Universe. In comparison, around 4.9% of the Universe is composed of SM matter, which cannot probe the dark sector. The dark energy is assumed to be an intrinsic constant energy density of the vacuum that affects the acceleration of the Universe. The study of large scale structures helps to understand the nature of dark energy [38]. The observational evidence of dark matter comes from gravitational lensing, cosmic microwave background (CMB), the evolution of the galaxies and galaxy clusters. These observations indicate the dark matter particles to be non-baryonic and non-relativistic, known as cold dark matter [39, 40]. The most favourable candidates for the non-baryonic cold dark matter are the weakly interacting massive particles (WIMP) [41, 42] and primordial black holes [43–45]. Since the SM is not able to explain the existence of these hypothetical particles, the BSM physics is essential to understand the dark sector.
- *Matter-antimatter asymmetry:* The predominance of matter over antimatter in the Universe is another puzzle inexplicable by the SM. Since the SM is constituted of both baryon and anti-baryons, it is naturally expected that the baryonic and anti-baryonic matter density should be equal. The baryon asymmetry parameter is defined as  $\eta_B = (n_B - \bar{n}_B)/n_\gamma$  with  $n_B$ ,  $\bar{n}_B$  and  $n_\gamma$  being the respective number densities of baryon, anti-baryon and photons. From the measurement of temperature anisotropy of the CMB radiation measured by Wilkinson Microwave Anisotropy Probe (WMAP) this asymmetry parameter is estimated to be  $\eta_B \sim 10^{-10}$  [46], which is also consistent with the analysis of the big bang nucleosynthesis [47]. The non-zero value of  $\eta_B$  clearly indicates the existing asymmetry between matter and antimatter in the Universe.

In order to explain the matter-antimatter asymmetry, in 1967 the three necessary conditions were developed by Sakharov [48],

- Baryon number violation
- Violation of C and CP symmetry
- Deviation from the thermal equilibrium

Even though the CP violation occurs within the framework of SM in terms of the complex phase appearing in the quark mixing matrix, as shown in Section 1.2, its current estimation does not suffice for the observed baryonic asymmetry. Therefore, new physics is required as

an explanation for the observed matter-antimatter asymmetry of the Universe, which might provide additional sources of the CP violation.

- *Neutrino oscillation:* One of the primary evidences of the existence of BSM physics is the discovery of neutrino flavour oscillation. The phenomenon of neutrino oscillation ( $\nu_\alpha \rightarrow \nu_\beta$ ) predicts the existence of small neutrino mass which is in sharp contrast with the SM. Since the SM does not include RH neutrino, the neutrinos remain massless in SM. The quantum mechanical theory of neutrino oscillation predicts the mixing between the neutrino flavour states and non-degenerate massive states, similar to the quark mixing as discussed in Section 1.2. However, the neutrino mixing angles are much larger as compared to the quark mixing angles. The neutrino oscillation gives rise to the concept of lepton flavour violation (LFV) which is strictly forbidden in SM. Therefore, one has to look for physics beyond SM to explain the neutrino oscillation. The details of the neutrino oscillation are discussed in the Section 1.3.

### 1.2.2 Neutrino in SM and beyond

The neutrino plays a dominant role in various domains of particle physics as well as in astrophysics and cosmology. The neutrino is the only elementary particle in SM that is involved in the weak interaction alone. The neutrinos were generated in copious amount at the time of the Big Bang and are now the second most abundant particle in the Universe. The neutrinos were decoupled from the thermal bath after  $\sim 1$  second of the birth of the Universe, when the temperature of its surroundings was  $\sim 1$  MeV. These Big Bang neutrinos are known as the relic neutrinos which form the cosmic neutrino background with the density  $\sim 336/\text{cc}$  and is existing at a temperature  $T_\nu \sim 1.9$  K. The detection of the relic neutrinos is very difficult because of its extremely small scattering cross section with matter. At present neutrinos are produced from various astrophysical objects such as supernova remnants and neutron stars which play a significant role in heat transport of the stellar systems. The sun also emits lower energy ( $\sim \text{MeV}$ ) neutrinos extensively during the nuclear fusion of hydrogen occurring inside its core. The particle accelerators and reactors on Earth can also produce neutrinos, with energies ranging from several  $\sim \text{MeV}$  up to a few  $\sim \text{GeV}$ .

In the SM framework, the neutrino is electrically neutral and massless fermion with fixed helicity, because of the absence of its RH counterpart. Shortly after the establishment of Dirac's theory of four component spinors for spin-1/2 relativistic particles, Weyl came up with his theory of two component spinors for massless particles in 1929 [49]. Since Weyl's theory showed the violation of the parity symmetry, which was assumed to be an exact symmetry of nature at that time, the idea of two component spinor was rejected. After the observation of maximal parity violation in Wu's experiment in 1957 [6], the two component theory of neutrino was proposed by several physicists [50–53]. The fermion field itself is represented as the sum of its LH and RH counterpart, given by  $\psi = \psi_L + \psi_R$ . The LH and RH projections of the field are represented as

$$\begin{aligned}\psi_L &= P_L \psi = \frac{(1 - \gamma_5)}{2} \psi, \\ \psi_R &= P_R \psi = \frac{(1 + \gamma_5)}{2} \psi.\end{aligned}\tag{1.8}$$

Here  $\gamma_5$  is the Chirality operator,  $\gamma_5 = i\gamma_0\gamma_1\gamma_2\gamma_3$ . In SM the neutrinos appear in three flavours,  $\nu_e$ ,  $\nu_\mu$  and  $\nu_\tau$ , each associated with individual lepton numbers,  $L_e$ ,  $L_\mu$  and  $L_\tau$ . The lepton numbers are opposite for the neutrino and anti-neutrino. The conservation of the lepton number is an accidental global symmetry of the SM, as a consequence of which the neutrinos in SM are massless. A massless neutrino always travels with the speed of light, and hence has a definite state of helicity irrespective of any frame of reference. The Weyl neutrino can be understood as a massless Dirac fermion. In most of the BSM scenarios, the neutrino acquires a small mass. The current upper bound of neutrino mass obtained from the KATRIN experiment is  $m_\nu < 0.8$  eV [54]. In the Dirac picture,

the neutrino and anti-neutrino are two distinguished particles with opposite helicities. Under the discrete CPT transformation, a LH Dirac neutrino is converted into a RH anti-neutrino. In the minimally extended SM, the neutrino is allowed to possess a small Dirac mass which occurs due to the inclusion of the right handed (RH) neutrino that interacts with the Higgs field via Yukawa interaction similar to the rest of the SM quarks and leptons.

$$\mathcal{L}_{mass}^{Dirac} = -m\nu\bar{\nu} = -m\bar{\nu}_R\nu_L + h.c. \quad (1.9)$$

However, if the neutrinos acquire purely Dirac mass, the corresponding Yukawa couplings are extremely small ( $\sim 10^{-12}$ , for neutrino mass to be  $\sim 0.1$  eV [55]), in comparison with the other SM fermions. This also requires the lepton number as a fundamental symmetry in the SM, although the global symmetry of lepton number is an accidental symmetry in SM. In 1937, an alternative approach was developed by Ettore Majorana in 1937 in which the neutrino and anti-neutrino are considered to be the same particle  $\nu = \nu^C$  [56, 57],  $\nu^C$  representing the charge-conjugated state. This implies that in Majorana formalism the LH and RH components of neutrino are connected by,  $\nu_R = \nu_L^C$ , unlike the case of Dirac neutrino, in which the chiral components are independent. Thus, the Majorana mass can be represented in terms of a single specific chiral neutrino as

$$\mathcal{L}_{mass}^{Majorana} = -\frac{1}{2}m\bar{\nu}_L^C\nu_L + h.c. \quad (1.10)$$

The Majorana mass cannot be generated from the renormalizable SM Lagrangian. Therefore, one has to go beyond SM to generate Majorana mass of neutrino, in which higher dimensional operators can be introduced. The lowest dimensional term that can generate Majorana mass for the neutrinos is the dimension-5 non-renormalizable Weinberg operator. After the EW symmetry breaking the dimension-5 operator can produce the Majorana mass which is restricted by the NP scale. Whether a neutrino is a Dirac or Majorana particle, is an open question in particle physics.

Neutrinos are one of the most promising candidates to search for BSM physics. There are several BSM scenarios involving neutrino physics which are discussed below.

1. *New interactions of neutrino:* The presence of physics beyond SM expects the neutrino to experience new interactions that are not usually seen in SM. This is manifested in terms of higher dimensional non-renormalizable operators made out of SM fields. These operators provide the effective description of new physics at the EW scale. The knowledge of such BSM physics can be perceived without constructing any specific model. The model independent NP incorporated in the neutrino sector is known as non-standard interaction (NSI). In addition to the SM interactions, the NSI imposes an extra sub-dominant effect which can alter the scenario of neutrino oscillation, as well as the neutrino scattering in matter. If NSI is present, the precise determination of standard neutrino oscillation parameters can be interrupted in the precision experiments. Although NSI can be present in both CC and NC interactions, for studying the neutrino interactions in matter, NC NSI is more relevant which is also the theme of this thesis. There are a broad number of models developed to generate NSI, in which the strength of the NSI depends on the mass of the mediator. The phenomenological consequences of the heavy and light mediators in describing NSI are completely different. The details of NSI are discussed in Chapter 2.
2. *Neutrino decay:* A possible BSM scenario in the neutrino sector is the decay of neutrino mass state  $\nu_i \rightarrow \nu_j + \phi$ . The neutrino decay is divided into two categories, visible and invisible decay. In case of the invisible decay, the final decay products are undetectable at the experiments. This is because either the decay product is a light sterile neutrino, or it is an active neutrino flavour having very low energy which might not be detected within the energy range of experiment. On the other hand, in case of visible decay, the decay products are lower energy active neutrino flavour states observable by the detector. From the phenomenological

perspective, the invisible decay results in the depletion in the number of neutrino events as compared to the SM prediction, while several lower energy regenerated neutrino events are expected in case of visible decay. The fraction of neutrinos decaying after traveling a distance  $L$  is expressed as the exponential damping factor  $e^{-m_i L/\tau_i E}$ ,  $E$  being the neutrino energy.  $m_i$  and  $\tau_i$  denote the mass of the mass eigenstate  $\nu_i$  and its lifetime respectively.

The constraints on neutrino decay are determined from several astrophysical and experimental observations. For visible decay an upper bound of  $\tau_2/m_2, \tau_3/m_3 \lesssim 10^{10}$  s/eV is obtained from supernova relic neutrino observation. The constraint estimated from the observation of supernova SN1987A is  $\tau/m > 10^5$  s/eV, considering only one massive neutrino state [58]. From the analysis of T2K and NO $\nu$ A data constrains  $\tau_3/m_3 > 2.8 \times 10^{-12}$  s/eV [59]. The constraint on neutrino decay is expressed as  $\tau_i/m_i$ , as the absolute neutrino mass scale is still unknown.

3. *Neutrino magnetic moment*: In SM the neutrinos are massless fermions, hence they do not exhibit any electromagnetic properties. However, the presence of its small non-zero mass can establish coupling between the neutrino and the magnetic field. In minimally extended SM if the neutrinos are Dirac fermions, the neutrino acquires magnetic moment through radiative corrections via quantum loop effect. Due to the small mixing between LH and RH counterparts, this magnetic moment is extremely small ( $\sim 10^{-19} \mu_B$ ) [60]. The Majorana neutrinos gain only off-diagonal magnetic moment having the order  $\sim 10^{-23} \mu_B$ . The current bound on the neutrino magnetic moment is much larger than these theoretical predictions ( $\sim 10^{-12} - 10^{-10} \mu_B$ ) [61–64]. The current upper bound of the magnetic moment estimated by XENONnT experiment is  $\sim 6.4 \times 10^{-12} \mu_B$  [65, 66], which is also consistent with the astronomical predictions. The non-standard interaction can induce neutrino magnetic moment [67–69].
4. *Right handed neutrino*: The idea of a fourth neutrino state was born to solve the excess  $\bar{\nu}_e$  events observed in short baseline (SBL) reactor experiment LSND [70]. Similar results were observed in  $\bar{\nu}_\mu \rightarrow \bar{\nu}_e$  channel in the MiniBooNE experiment at Fermilab [71]. It was pointed out that by incorporating one additional RH sterile neutrino with the SM neutrino states, these two anomalies are resolved [72, 73]. Theoretically, in the simplest extension of the SM, an additional RH neutrino is incorporated in the SM. The inclusion of the RH components with the LH neutrinos affects the CC interaction, which gives rise to the non-unitary feature of the mixing matrix. If there are  $n$  number of neutrinos, the general mixing matrix is larger than  $3 \times 3$  which is given by

$$\mathcal{U} = \begin{pmatrix} N^{3 \times 3} & \Theta^{3 \times (n-3)} \\ R^{(n-3) \times 3} & S^{(n-3) \times (n-3)} \end{pmatrix} \quad (1.11)$$

Here  $N^{3 \times 3}$  is the non-unitary matrix for the mixing in the LH neutrino sector.  $\Theta$  represents the mixing between the active and heavy states.  $R$  and  $S$  denote the mixing of the sterile states with the light and heavy states respectively. One standard parametrization of the non-unitary mixing matrix is given by [74, 75]

$$N^{3 \times 3} = \begin{pmatrix} 1 - \alpha_{ee} & 0 & 0 \\ \alpha_{\mu e} & 1 - \alpha_{\mu\mu} & 0 \\ \alpha_{\tau e} & \alpha_{\tau\mu} & 1 - \alpha_{\tau\tau} \end{pmatrix} U. \quad (1.12)$$

Here  $U$  is the  $3 \times 3$  unitary mixing matrix in the LH neutrinos.  $\alpha_{ij}$  are non-unitary parameters. In the limit  $\alpha_{ij} \rightarrow 0$ , the unitarity is restored. The mass scale of this additional state results in compelling phenomenological consequences. If the mass of the RH neutrino state is above the EW scale, it cannot be produced in the neutrino beam of oscillation experiments. In that

case, the mixing between the flavour and mass basis is connected by only  $N^{3 \times 3}$ , given by (1.12). In this case, the flavour states no longer remain orthonormal. On the other hand, if the right handed neutrino is light enough to be produced in the neutrino beam used in the neutrino experiments, it generates new oscillation frequencies and takes part in the neutrino oscillation phenomena. In this scenario, the mixing scenario is explained by the total mixing matrix given by  $\mathcal{U}$  in Eqn. (1.11).

As discussed in Section 1.2.1, neutrino oscillation is an integral part of neutrino physics and one of the foremost signatures of the existence of the physics beyond SM. The phenomenology of neutrino oscillation is described in the following sections.

## 1.3 Neutrino oscillation

Neutrino oscillation is a quantum mechanical phenomenon that can only occur if the neutrino has a small non-zero mass. Neutrinos are produced in three different flavors in various experiments and astrophysical sources. Each flavour state is converted into the other flavour states while the neutrino propagates through the medium. In the neutrino detectors, the flavour of a neutrino can be specified, but its mass cannot be predicted, as the flavour states do not have definite mass. Therefore, a neutrino of a particular flavour can freely oscillate among all possible flavours states. In the next subsections, the phenomenon of neutrino oscillation is discussed in detail.

### 1.3.1 Brief history of neutrino oscillation

The idea of neutrino oscillation was first introduced by Pontecorvo in 1957 after the discovery of the oscillation of the strange quantum number in the neutral  $K$ -meson system  $K^0 \rightleftharpoons \bar{K}^0$ . Soon after the establishment of the two component theory of neutrino [51], Pontecorvo published a paper describing the idea of the neutrino oscillation in 1958 [76]. Since only one type of neutrino was known at that time, the mixing between neutrino and anti-neutrino was considered. In 1962, after the discovery of  $\nu_\mu$  the concept of the neutrino mass and mixing was further instigated by Maki, Nakagawa and Sakata [77]. In 1967, Pontecorvo discussed about the solar neutrinos and pointed out that the reduction in the solar neutrino flux was caused by the neutrino flavour oscillation  $\nu_\mu \rightleftharpoons \nu_e$  [78].

In the late 1960s astrophysicists Raymond Davis and John Bahcall measured the flux of solar neutrinos produced by the nuclear fusion occurring inside the sun at an experiment in Homestake mine in South Dakota using a chlorine-rich target  $^{37}\text{Cl} + \nu_e \rightarrow ^{37}\text{Ar} + e^-$ . The observed flux was found to be about three times smaller than the predicted value from the standard solar model [79]. This is widely known as the *solar neutrino problem (SNP)*. This was resolved with the phenomenon of neutrino oscillation according to which the missing solar neutrinos  $\nu_e$  are converted to another active flavour state  $\nu_\mu$  along their way to Earth. Since the Homestake experiment was unable to detect the  $\nu_\mu$ , it seemed at that time that some of the incoming neutrinos are disappeared. Later the flux deficit in solar neutrino was also observed in the gallium experiments namely, GALLEX/GNO [80] and SAGE [81] and water cherenkov detectors such as Kamiokande [82] and Sudbury Neutrino Observatory (SNO) [83]. In 2001 the result from SNO presented the first evidence of neutrino oscillation in the solar neutrinos confirming the large mixing angle (LMA) solution [83, 84]. The reactor neutrino experiment KamLAND observed the  $\bar{\nu}_e$  flux emitted from nuclear reactors to address the SNP under the laboratory conditions and also confirmed the LMA solution of the neutrino oscillation [85].

The signature of neutrino oscillation was also evident from the anomaly observed in the atmospheric neutrino flux. The atmospheric neutrinos are produced by the interaction of the cosmic

ray particles arriving on Earth from outer space with the nuclei present at the top of the atmosphere. In 1965 the atmospheric neutrinos were detected for the first time by the underground neutrino detectors in South India [86] and South Africa [87]. In the late 1980s the atmospheric  $\nu_\mu$  flux was found to be much smaller than its SM prediction. This was confirmed at Irvine–Michigan–Brookhaven (IMB) [88, 89] and Kamiokande neutrino detectors [90–92] and is known as the *atmospheric neutrino anomaly*. In 1998 the problem of the observed flux deficit was resolved at Super Kamiokande (SK) experiment with the confirmation of the flavour oscillation in atmospheric neutrinos from  $\nu_\mu$  to  $\nu_\tau$  [93]. In 2015, Japanese Physicist Taakaki Kajita shared the Nobel Prize in Physics for his contribution to the SK experiment, with Arthur McDonald who was the director of the SNO experiment.

### 1.3.2 Neutrino oscillation in vacuum

The neutrinos are produced in three different flavours  $\nu_e, \nu_\mu, \nu_\tau$  which are also known as weak eigen states since the neutrinos only participate in the weak interaction. Although the neutrinos are produced as flavour states, they travel as the superposition of the three mass eigenstates  $\nu_1, \nu_2, \nu_3$ . The mass eigenstates are stationary and non-degenerate which do not oscillate among each other. The flavour ( $\nu_f$ ) and mass eigenstates ( $\nu_m$ ) of neutrino are connected by a unitary operator ( $U$ ) given by

$$|\nu_\alpha\rangle = U |\nu_i\rangle \implies \begin{pmatrix} |\nu_e\rangle \\ |\nu_\mu\rangle \\ |\nu_\tau\rangle \end{pmatrix} = U \begin{pmatrix} |\nu_1\rangle \\ |\nu_2\rangle \\ |\nu_3\rangle \end{pmatrix}.$$

The above equation represents the flavour states as the linear superposition of the mass eigenstates. It is to be mentioned that both the flavour and mass basis vectors are orthonormal *i.e.*  $\langle\nu_\alpha|\nu_\beta\rangle = \delta_{\alpha\beta}$ ,  $\langle\nu_i|\nu_j\rangle = \delta_{ij}$ . The time evolution of the mass eigenstates is given by

$$|\nu_i(t)\rangle = e^{-iH_i t} |\nu_i(0)\rangle, \quad (1.13)$$

where  $H_i$  is the Hamiltonian corresponding to the mass basis. The mass eigen states  $\nu_i$  follow the dispersion relation  $E_i = \sqrt{\mathbf{p}_i^2 + m_i^2}$  which implies that all the massive states possess different momenta [94] and they propagate in the same direction while traveling from the source to the detector. At any time  $t$ , the flavour eigenstate is expressed as the linear combination of the initial flavour states at  $t = 0$ , given by

$$|\nu_\alpha(t)\rangle = e^{-iH_f t} |\nu_\alpha(0)\rangle = U e^{-iH_m t} U^\dagger |\nu_\alpha(0)\rangle. \quad (1.14)$$

Here  $H_f$  represents the Hamiltonian for neutrino propagation in flavour basis. Thus, if at  $t = 0$  a neutrino is produced in the state  $|\nu_e\rangle$ , after traversing a certain distance in time  $t$ , the general neutrino state becomes a mixture of the three flavours. This also alters the mixture of mass eigenstates with time. The neutrino oscillation continues as long as the coherence is maintained in the system.

The unitary matrix connecting the flavour and mass basis in Eqn. (1.13) can be represented in terms of three mixing angles,  $\theta_{12}, \theta_{23}, \theta_{13}$  and a complex violating phase  $\delta$  which is known as PMNS phase and can be represented as follows

$$U(\theta_{12}, \theta_{23}, \theta_{13}, \delta) = \begin{pmatrix} c_{12}c_{13} & s_{12}c_{13} & s_{23}e^{-i\delta} \\ -s_{12}c_{23} - c_{12}s_{23}s_{13}e^{i\delta} & c_{12}c_{23} - s_{12}s_{23}s_{13}e^{i\delta} & s_{23}c_{13} \\ s_{13}s_{23} - c_{12}c_{23}s_{13}e^{i\delta} & -c_{12}s_{23} - s_{12}c_{23}s_{13}e^{i\delta} & c_{23}c_{13} \end{pmatrix}. \quad (1.15)$$

Here  $c_{ij} = \cos\theta_{ij}$  and  $s_{ij} = \sin\theta_{ij}$ . The complex phase  $\delta$  introduces CP violation in the neutrino sector. The flavour oscillation probability depends on the energy difference of the non-degenerate

mass eigenstates,  $E_i - E_j$  which, in the ultra-relativistic limit ( $E \approx p$ ), is given by

$$E_i - E_j \approx \frac{\Delta m_{ij}^2}{2E}, \quad (1.16)$$

where  $\Delta m_{ij}^2$  is the mass square difference. The neutrino oscillation experiments are consistent with this approximation since the experiments are operated at energy in the  $\sim$ MeV-GeV range, which is much higher than the mass of the neutrino ( $\sim$  few eV). Also, the experimental facilities measure the propagation length between the source and the detector  $L$  instead of the time  $t$  which is compatible with the consideration of the ultra-relativistic limit. With this consideration, the expression of the flavour transition probability is given by

$$\begin{aligned} P_{\nu_\alpha \rightarrow \nu_\beta} &= \sum_{i,j} U_{\alpha i}^* U_{\beta j} U_{\alpha j} U_{\beta j}^* \exp\left(\frac{-i\Delta m_{ij}^2 L}{2E}\right) \\ &= \sum_{i,j} U_{\alpha i}^* U_{\beta j} U_{\alpha j} U_{\beta j}^* \exp\left(\frac{-2\pi i L}{L_{ij}^{osc}}\right), \end{aligned} \quad (1.17)$$

where  $L_{ij}^{osc} = 4\pi E / \Delta_{ij}^2$  is the oscillation length, defined as the distance at which the phase generated by  $\Delta m_{ij}^2$  becomes  $2\pi$ . To observe the flavour oscillation occurring because of the interference of the massive states, the production and detection processes at the neutrino experiments must be confined in a region smaller than the oscillation length  $L_{ij}^{osc}$  [95]. This condition is achieved by all the oscillation experiments. The neutrino oscillation probability in Eqn. (1.17) can also be represented in the following form by separating the real and imaginary components

$$\begin{aligned} P_{\nu_\alpha \rightarrow \nu_\beta} &= \delta_{\alpha\beta} - 4 \sum_{i>j} \text{Re}(U_{\alpha i}^* U_{\beta i} U_{\alpha j} U_{\beta j}^*) \sin^2\left(\frac{\Delta m_{ij}^2 L}{4E}\right) \\ &\quad + 2 \sum_{i>j} \text{Im}(U_{\alpha i}^* U_{\beta i} U_{\alpha j} U_{\beta j}^*) \sin\left(\frac{\Delta m_{ij}^2 L}{2E}\right). \end{aligned} \quad (1.18)$$

In case of anti-neutrino, the above expression of the oscillation probability only differs in the sign of the imaginary part and is represented as

$$\begin{aligned} P_{\bar{\nu}_\alpha \rightarrow \bar{\nu}_\beta} &= \delta_{\alpha\beta} - 4 \sum_{i>j} \text{Re}(U_{\alpha i}^* U_{\beta i} U_{\alpha j} U_{\beta j}^*) \sin^2\left(\frac{\Delta m_{ij}^2 L}{4E}\right) \\ &\quad - 2 \sum_{i>j} \text{Im}(U_{\alpha i}^* U_{\beta i} U_{\alpha j} U_{\beta j}^*) \sin\left(\frac{\Delta m_{ij}^2 L}{2E}\right). \end{aligned} \quad (1.19)$$

The oscillation length  $L_{osc}^{ij}$  remains the same in case of both neutrino and anti-neutrino.

In the three flavour neutrino oscillation scenario, there appear three mass squared differences  $\Delta m_{21}^2$ ,  $\Delta_{31}^2$  and  $\Delta m_{32}^2$ , out of which the smaller and larger mass squared differences  $\Delta m_{21}^2$  and  $\Delta m_{31}^2$ ,  $\Delta m_{32}^2$  are associated with the solar and atmospheric neutrinos respectively. It is well established from the observation of the solar neutrino that the sign of  $\Delta m_{21}^2$  is positive for the neutrino and negative for the anti-neutrino, implying the fact that  $\nu_2$  is heavier than  $\nu_1$ . However, the position of the third mass eigen state  $\nu_3$  is not known. If it is heavier than  $\nu_1$  and  $\nu_2$ ,  $\Delta m_{31}^2$  is positive, which is known as normal mass ordering (NO). The reverse case is known as inverted mass ordering (IO) in which the sign of  $\Delta m_{31}^2$  is negative. The details of mass hierarchy is illustrated in Fig. 1.2. Currently ongoing accelerator and reactor experiments are trying to resolve this mass hierarchy problem. The correct estimation of the leptonic CP violating phase  $\delta$  is also still unknown. The CP transformation interchanges neutrino and antineutrino *i.e.*  $\nu_\alpha \xleftrightarrow{\text{CP}} \bar{\nu}_\alpha$ . The neutrino flavour

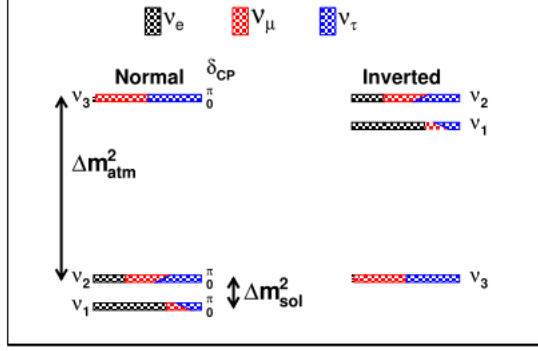


**Figure 1.2:** Neutrino mass hierarchy

oscillation transforms under the CP operator as,  $\nu_\alpha \rightarrow \nu_\beta \xleftrightarrow{\text{CP}} \bar{\nu}_\alpha \rightarrow \bar{\nu}_\beta$ . In neutrino oscillation experiments, the extent of CP violation is measured in terms of the CP asymmetry parameter which is defined as the difference between the neutrino and anti-neutrino oscillation probabilities, given by

$$A_{\alpha\beta}^{CP}(L, E) = P_{\nu_\alpha \rightarrow \nu_\beta} - P_{\bar{\nu}_\alpha \rightarrow \bar{\nu}_\beta} = 4 \sum_{i>j} \text{Im}(U_{\alpha i}^* U_{\beta i} U_{\alpha j} U_{\beta j}^*) \sin\left(\frac{\Delta m_{ij}^2 L}{2E}\right). \quad (1.20)$$

Due to the imposition of the CPT symmetry ( $\nu_\alpha \rightarrow \nu_\beta \xleftrightarrow{\text{CPT}} \bar{\nu}_\beta \rightarrow \bar{\nu}_\alpha$ ), the CP asymmetry parameter is antisymmetric in flavour  $A_{\alpha\beta}^{CP} = -A_{\beta\alpha}^{CP}$ . Eqn. (1.20) implies that the measurement of CP asymmetry is only possible by observing the flavour transitions in the neutrino oscillation experiments. Also, the baseline length and the energy range of the experimental facilities should be fixed in such a way that the argument  $\Delta m_{ij}^2 L/2E$  is not too small for the parameter  $A_{\alpha\beta}^{CP}$  to be measured. On the other hand, if  $\Delta m_{ij}^2 L/2E$  is too large, it results in the asymmetry parameter to be zero as the uncertainties in  $L$  and  $E$  are averaged out. Although the three flavour neutrino oscillation provides the complete description of the flavour transition, it can be reduced to an effective two flavour scenario which is relevant for the neutrino oscillation experiments. In two flavour neutrino oscillation is an approximation in which only two massive states are considered. The mathematical expression of the probabilities is much simpler in the two flavour scenario as it involves a lesser number of parameters, one mixing angle and one mass squared difference. Here, the flavour and mass eigenstates are related by a  $2 \times 2$  rotation matrix, given by

$$\begin{pmatrix} \nu_\alpha \\ \nu_\beta \end{pmatrix} = \begin{pmatrix} \cos\theta & \sin\theta \\ -\sin\theta & \cos\theta \end{pmatrix} \begin{pmatrix} \nu_1 \\ \nu_2 \end{pmatrix}. \quad (1.21)$$

The expression of the oscillation probability is represented as

$$P_{\nu_\alpha \rightarrow \nu_\beta} = \sin^2 2\theta \sin^2\left(\frac{\Delta m^2 L}{4E}\right). \quad (1.22)$$

From the above equation, it is clear that the survival probability remains unchanged under the transformation of the mixing angle from  $\theta$  to  $\pi/2 - \theta$ . Such degeneracy implies that there can be two possible solutions of the oscillation probability corresponding to the mixing angles in two different octants,  $\theta < \pi/4$  and  $\theta > \pi/4$ . The mixing of the different mass eigenstates for a particular neutrino flavour becomes different for the two degenerate solutions. For example, if  $\theta < \pi/4$ , it means

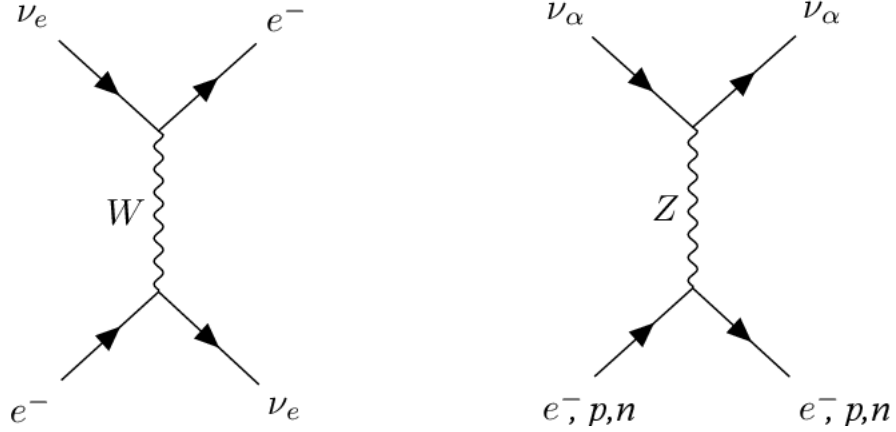


**Figure 1.3:** Charged (CC) and neutral current (NC) interactions of neutrino in SM

that  $\nu_e$  is composed more of  $\nu_1$  as compared to  $\nu_2$ , while for  $\theta > \pi/4$ , the contribution of  $\nu_2$  is greater than  $\nu_1$ . Further, there is no CP violation in the two flavour oscillation scenario which implies that the flavour transition probabilities of neutrino and anti-neutrino are equal,  $P_{\nu_\alpha \rightarrow \nu_\beta} = P_{\bar{\nu}_\alpha \rightarrow \bar{\nu}_\beta}$ .

### 1.3.3 Neutrino oscillation in matter

When the neutrino travels through the matter, it is subjected to a potential due to the presence of different matter particles and undergoes coherent forward elastic scattering. Such interaction alters the mixing among the mass eigenstates  $P_{\alpha \rightarrow \beta}$ . This was established by L. Wolfenstein in 1978 [96]. The neutrino propagating in the matter is also influenced by the incoherent scatterings with the surrounding particles. However, the mean free path associated with the incoherent scattering events is extremely large in Earth's matter density, even much larger than the diameter of the Earth. Therefore, the effect of such scattering is safely neglected while determining the neutrino oscillation probabilities in the terrestrial experiments [95]. The effect of incoherent scattering is only relevant for the highly dense environment in compact astrophysical objects, such as neutron stars.

When an active flavour of neutrino propagates through the matter, it interacts with the constituent particles via weak charged current (CC) and neutral current (NC) interactions which affect its evolution. In SM the CC interaction is mediated by the weak vector boson  $W^\pm$ , while the NC interaction takes place by the exchange of  $Z^0$  boson. Considering the neutrino interactions in Earth matter which consists of only electron, proton and neutron,  $\nu_e$  can undergo both CC and NC interactions, while  $\nu_\mu$  and  $\nu_\tau$  only experience NC interaction. The scattering process  $\nu_e e^- \rightarrow \nu_e e^-$  can be mediated by both  $W$  and  $Z$ -boson, while the interaction with the nucleons always occurs via the NC channel. The CC interaction of  $\nu_\mu$  or  $\nu_\tau$  is given by inverse muon decay  $\nu_\mu(\tau) e^- \rightarrow \mu(\tau) \nu_e$ . This interaction does not retain the identity of the initial particles, unlike  $\nu_e - e$  scattering. The Lagrangian for the CC weak interaction for the process  $\nu_e e^- \rightarrow \nu_e e^-$  is given by

$$\mathcal{L}_{CC} = \frac{G_F}{\sqrt{2}} [\bar{\nu}_e(x) \gamma^\mu P_L e(x)] [\bar{e}(x) \gamma_\mu P_L \nu_e(x)], \quad (1.23)$$

and that for the NC interaction is given by

$$\mathcal{L}_{NC} = \frac{G_F}{\sqrt{2}} \sum_{\alpha=e,\mu,\tau} [\bar{\nu}_\alpha(x) \gamma^\mu P_L \nu_\alpha] [\bar{f}(x) \gamma_\mu (g_V^f - g_A^f \gamma_5) f(x)]. \quad (1.24)$$

Here  $G_F$  is the Fermi constant. The potentials experienced by the  $\nu_e$  due to the CC and NC

reactions can be calculated using Feynmann rules which are expressed as

$$\begin{aligned} V_{CC} &= \sqrt{2}G_F N_e, \\ V_{NC} &= -\frac{1}{\sqrt{2}}G_F N_n. \end{aligned} \quad (1.25)$$

In the case of NC potential the contribution due to the electrons and protons cancel out each other due to the charge neutrality criteria of the matter, hence the only contribution comes from the neutrons. This results in a common phase factor which can be safely neglected while calculating the oscillation probability. The Hamiltonian of neutrino oscillation in the presence of matter effect in the flavour basis is expressed as

$$\begin{aligned} H_f &= H_0 + H_I \\ &= U \begin{pmatrix} 0 & 0 & 0 \\ 0 & \Delta m_{21}^2/2E & 0 \\ 0 & 0 & \Delta m_{31}^2/2E \end{pmatrix} U^\dagger + \begin{pmatrix} V_{CC} & 0 & 0 \\ 0 & 0 & 0 \\ 0 & 0 & 0 \end{pmatrix}. \end{aligned} \quad (1.26)$$

The sign of the matter potential  $V_{CC}$  is '+ve' for neutrino and '-ve' for anti-neutrino. In the presence of matter effect, the vacuum mass eigenstates are modified which alters the mixing angle and the mass squared difference associated with the oscillation in vacuum. In the two flavour scenario, the effective mass squared difference  $\Delta m_M^2$  and mixing angle  $\theta_M$  considering the matter effect are given by

$$\begin{aligned} \Delta m_M^2 &= \sqrt{(\Delta m^2 \cos 2\theta - 2EV_{CC})^2 + \Delta m^2 \sin^2 2\theta} \\ \sin^2 2\theta_M &= \frac{\sin^2 2\theta}{\sin^2 2\theta + (\cos 2\theta - V_{CC})^2}. \end{aligned} \quad (1.27)$$

The mixing matrix, given in Eqn. (1.21), is also modified as

$$U_M = \begin{pmatrix} \cos\theta_M & \sin\theta_M \\ -\sin\theta_M & \cos\theta_M \end{pmatrix}.$$

The form of the expression of the neutrino flavour transition probability remains the same as that obtained in case of oscillation in vacuum, given by Eqn. (1.22), only with the mass squared difference  $\Delta m^2$  and the mixing angle  $\theta$  are replaced by  $\Delta m_M^2$  and  $\theta_M$  respectively, so that the oscillation probability is represented as

$$P_{\nu_\alpha \rightarrow \nu_\beta}^M = 1 - \sin^2 2\theta_M \sin^2 \left( \frac{\Delta m_M^2 L}{4E} \right). \quad (1.28)$$

The octant degeneracy in the mixing angle solution, discussed in Subsection 1.3.2, is lifted in presence of matter effect.

### 1.3.4 Neutrino oscillation experiments

The currently ongoing neutrino oscillation experiments are measuring the mixing parameters with unprecedented precisions that can provide a more comprehensive understanding of the unknowns (*e.g.* CP violating phase  $\delta$ , octant of  $\theta_{23}$ , sign of the larger mass square difference  $\Delta m_{32}^2$ ) in the neutrino oscillation paradigm. The experimental facilities are designed to detect the oscillation phenomena based on two techniques

- Appearance experiments, in which if the neutrino is produced in a particular flavour in the source (say,  $\nu_\alpha$ ), a different flavour is searched for in the detector.

- Disappearance experiments, in which the survival probability of a neutrino flavour is observed, *i.e.* the number of neutrinos produced in a specific flavour is compared with the number of the same flavour of neutrino measured at the detector.

The neutrino beam used in different appearance and disappearance experiments can be generated from the particle accelerators or reactors which are discussed below.

- *Reactor experiments:* The neutrino beam generated in reactor experiments is made up of  $\bar{\nu}_e$  produced from the beta decay reactions ( $\bar{\nu}_e + p \rightarrow n + e^+$ ) of the heavy unstable fission nuclei ( $^{235}\text{U}$ ,  $^{238}\text{U}$ ,  $^{239}\text{Pu}$ ,  $^{241}\text{Pu}$ ). The reactor neutrinos are emitted with an energy range of the order of a few MeV. The examples of a few reactor experiments with short baseline (SBL)  $L \lesssim 50$  km are Daya Bay, Double Chooz and RENO. These SBL reactor experiments are sensitive to the parameters  $\theta_{13}$ . In 2013, the bound on  $\theta_{13}$  was presented by the RENO collaboration  $\sin^2 2\theta_{13} = 0.100 \pm 0.010 \pm 0.015$  [97]. In 2014, the value of  $\theta_{13}$  was updated according to the result obtained from the Daya Bay experiment,  $\sin^2 2\theta_{13} = 0.084 \pm 0.005$  [98]. KamLAND experiment ( $L = 180$  km) has the longest baseline among the reactor experiments, which is sensitive to  $\theta_{12}$  and  $\Delta m_{21}^2$ . In 2008, KamLAND published the best fit values of these parameters,  $\tan^2 \theta_{12} = 0.56_{-0.07}^{+0.10}(\text{stat})_{-0.06}^{+0.10}(\text{syst})$  and  $\Delta m_{21}^2 = 7.58_{-0.13}^{+0.14}(\text{stat})_{-0.15}^{+0.15}(\text{syst}) \times 10^{-5} \text{ eV}^2$  [99].
- *Accelerator experiments:* The accelerator experiments were proposed to clarify the atmospheric neutrino anomaly. Here the  $\nu_\mu$  beam is generated from the decay of pions produced by colliding a high energy proton beam onto a target. The energy of the neutrino beam is usually within the range  $\sim 0.5 - 10$  GeV. This is comparatively larger than the energy restriction in the reactor experiments, hence the baseline lengths of the accelerator experiments are larger and these are sensitive to the larger mixing angle  $\theta_{32}$  and mass square difference  $\Delta m_{32}^2$ . DUNE is the longest baseline ( $L = 1300$  km) accelerator experiment with its near detector at Fermilab and the far detector at Sanford Lab in South Dakota. DUNE will start working from 2027 [100]. MINOS experiment ( $L = 735$  km) started working since 2005 and reported the measurements  $\sin^2 2\theta_{23} = 0.43_{-0.04}^{+0.2}$ ,  $\Delta m_{32}^2 = 2.40_{-0.09}^{+0.08} \times 10^{-3} \text{ eV}^2$  for NO and  $\sin^2 2\theta_{23} = 0.42_{-0.03}^{+0.07}$  and  $\Delta m_{32}^2 = 2.45_{-0.08}^{+0.07} \times 10^{-3} \text{ eV}^2$  for IO [101]. T2K is an LBL accelerator experiment ( $L = 295$  km) in Japan that recently presented updated constraints on the oscillation parameters  $\sin^2 2\theta_{23} = 0.561_{-0.032}^{+0.021}$  and  $\Delta m_{32}^2 = 2.494_{-0.058}^{+0.041} \times 10^{-3} \text{ eV}^2$  [102].

## 1.4 Overview of the thesis

The neutrino plays a vital role to look for physics beyond SM. Starting from the establishment of the neutrino flavour oscillation and the prediction of its non-zero mass, neutrino physics is proven to be a profound platform to provide insights into BSM physics. The signature of NP can be manifested in both lower and higher energy domains. This thesis includes the study of two such NP scenarios at the two extreme energy domains. The unambiguous signal of NP that is restricted in SM, can be incorporated in the neutrino sector in a model independent way, known as the non-standard interaction (NSI). If the NSI is present, it alters both the neutrino oscillation probability and its scattering cross section in matter. At present, both the oscillation and scattering experiments are sensitive to NSI and hence, they can provide paramount insights about it.

The neutrino oscillation is a quantum mechanical phenomenon. The quantumness embedded in the neutrino system can be quantized in terms of different quantum correlation measures which are an integral part of the quantum information sector. Several measures of quantum correlation can be written in terms of neutrino oscillation probabilities and are investigated in context of the neutrino oscillation experiments. The presence of NSI can alter the neutrino oscillation probabilities

and consequently the quantum correlations. This thesis includes one such study that includes the analysis of the NSI effect in the quantum correlation measures in the context of a long baseline accelerator experiment.

One of the possibilities of the NP in the ultra high energy regime is the production of exotic objects like microscopic black holes, which can be generated from the scattering of cosmic neutrinos inside the Earth. The signature of such unique events can be explored by the large underground neutrino telescopes. The second part of the thesis is based on the effect of NSI analysed in case of the black hole production.

The outline of the thesis is as follows. In Chapter 2, the NP scenarios studied in this thesis are discussed. First, the introduction of NSI is given starting with its effective field theoretical description. Then the concept of microscopic black hole is described in the presence of large extra dimensions and their production mechanism from the ultra high energy neutrino.

In Chapter 3, the basics of quantum correlation and its different measures are portrayed. The quantum correlation in the context of neutrino oscillation is also discussed.

In Chapter 4, the effect of NSI is studied in the temporal and spatial correlations in the context of the LBL neutrino oscillation experiment.

In Chapter 5, the NSI effect is studied in the production of the microscopic black holes from the ultra high energy neutrinos.

In Chapter 6, the conclusion of the thesis is presented along with the future direction. A brief description of the other works, which are not part of the thesis, is also given at the end of this chapter.